Chapter 7

Graphene Based Waveguides

Xianglian Song, Xiaoyu Dai and Yuanjiang Xiang

Additional information is available at the end of the chapter

http://dx.doi.org/10.5772/intechopen.76796

Abstract

Graphene, which is well known as a one-atom thick carbon allotrope, has drawn lots of attention since its first announcement due to remarkable performance in mechanical, electrical, magnetic, thermal, and optical areas. In particular, unique properties of graphene such as low net absorption in broadband optical band, notably high nonlinear optical effects, and gate-variable optical conductivity make it an excellent candidate for high speed, high performance, and broadband electronic and photonics devices. Embedding graphene into optical devices longitudinally would enhance the light-graphene interaction, which shows great potential in photonic components. Since the carrier density of graphene could be tuned by external gate voltage, chemical doping, light excitation, graphene-based waveguide modulator could be designed to have high flexibility in controlling the absorption and modulation depth. Furthermore, graphene-based waveguides could take advantages in detection, sensing, polarizer, and so on.

Keywords: graphene, waveguide, photonics, tunable, optical

1. Introduction

With the increasing demand in data storage, high-performance computing, and broadband networks for communication, the requirement for high-performance optical devices with broadband working bandwidth could be imaged [1–3]. Among the whole process, integrating telecom network onto chips has irreplaceable importance [4]. Since waveguide is one of the most indispensable components in modern communication, its development surely means a lot, which would otherwise impede the whole progress of optical technology [5]. Silicon photonics could provide broad bandwidths, which have been applied to low-loss optical waveguides [6, 7]. Other photonic substrates such as germanium or compound semiconductors are required to achieve high performance at the same time [4, 8]. However, the common

use of such materials is restricted due to limited bandwidth, inevitable cross-talk, high-energy consumption, expensive cost, and so on [9, 10].

Two-dimensional (2D) materials, such as graphene, black phosphorus (BP), hexagonal boron nitride (hBN), and transition metal dichalcogenides (MX_2, such as ReS_2, MoS_2, WS_2, WSe_2), have been of tremendous interest for applications in electronics, optoelectronics, and integrated photonics due to their unique and distinctive properties from bulk ones [11, 12]. Among all these 2D materials, graphene plays a special role in leading the exploration of 2D materials, which was first isolated mechanically in 2004 [13, 14]. Graphene, which is well known for thinnest, strongest, and highest mobility, shows great potential in various applications. Besides, graphene absorbs only ~2.3% in normally incident waves in and optical range, as shown in **Figure 1**, and the interaction of graphene with electromagnetic wave covers a broadband from the visible to terahertz spectral range [16, 17]. Remarkably, the conduction and valence bands in a mono layer graphene meet at direct, leading to a gapless and semi-metallic band structure, which could be adjusted by doping or some other external excitations [18–20].

The unique and extraordinary properties of graphene make it possible to be an ideal alternative in high-performance optoelectronic devices [21–25]. Hence, graphene, the unique 2D carbon atoms arranged in a honeycomb lattice, has been widely reported as an excellent plasmonic material for light-matter interactions from terahertz to the infrared (IR) region [18]. The gapless linear dispersion of Dirac fermions makes it possible for graphene integrated with other substrates to formulate modulators, polarizers, broadband waveguides, photodetectors, bio-sensors and so on [25–27]. Especially in the optical range, graphene-based waveguides play a critical role in photonic integrated circuits, optical fiber communication and sensing, as shown in **Figure 1**. It has been reported that coplanar integration which are planarized with

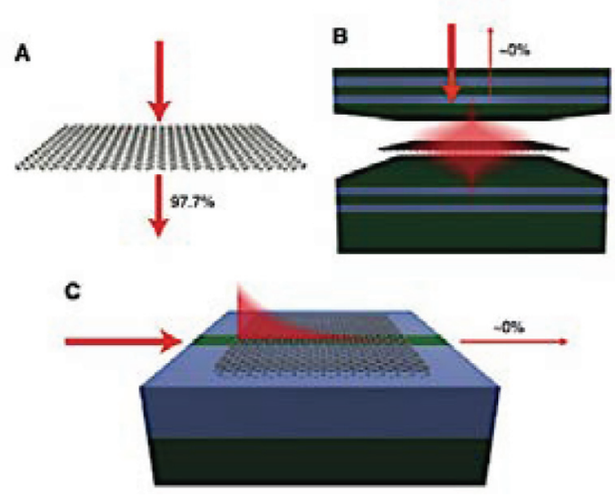

Figure 1. Different configurations for light-matter interaction in graphene. (A) For normal incident wave in optical range, graphene has the advantage of broadband absorption, the total absorption is quite small though. (B) When graphene is placed into an oical resonator, the absorption could be enhanced since the interaction between light and mater is enhanced. (C) When integrating graphene at the surface of photonics substrates, the interaction length would increase while the broadband optical bandwidth remains unchanged [15].

cladding materials could be achieved by transferring and the lamination of graphene to the surface of silicon photonic substrates. Integrating graphene with photonic devices not only promotes the emergence of novel optoelectronic properties but also opens a new versatile platform to investigate more fundamental application of graphene.

Three independent research groups, Mueller's group [28] at Vienna University of Technology and Johannes Kepler University (Australia), Englund's group [29] at Columbia University, the Massachusetts Institute of Technology (MIT) and the IBM T.J. Watson Research Center (the USA), and Xu's group [30] at Chinese University of Hong Kong (China), reported almost at the same time, chip-integrated graphene photodetectors with high responsivities and speeds, for which the working wavelength is covered from 1.3 to 2.75 μm [31]. Graphene-based photodetectors have better performance than germanium-based devices, because germanium-based ones meet limitations to overcome the low efficiencies at wavelength above 1.5 μm. However, this problem does not exist in graphene due to the zero-bandgap intrinsic property. As a result, the optical absorption coefficient remains constant from visible to infrared range owing to the linear band structure. Thus, a nearly flat response covering almost the whole optical communication band would not be out of image.

Pospischil and Mueller et al. [24] achieved a new kind of graphene-band optical interconnect, which owned an ultra-wideband operation from the O to the U band, as shown in **Figure 2**. Besides, the operation speed of graphene-based transition has been proved to be really high, which could be a perfect candidate for high-speed data transmission. Moreover, this device could overcome the biggest obstacles in conventional ones; the energy consumption in a graphene-based modulator is quite low. Due to the strong optical interaction in graphene, small devices in single chips were possible. The mechanical flexibility of graphene plays a role in formulating active components in polymer-based optical circuits.

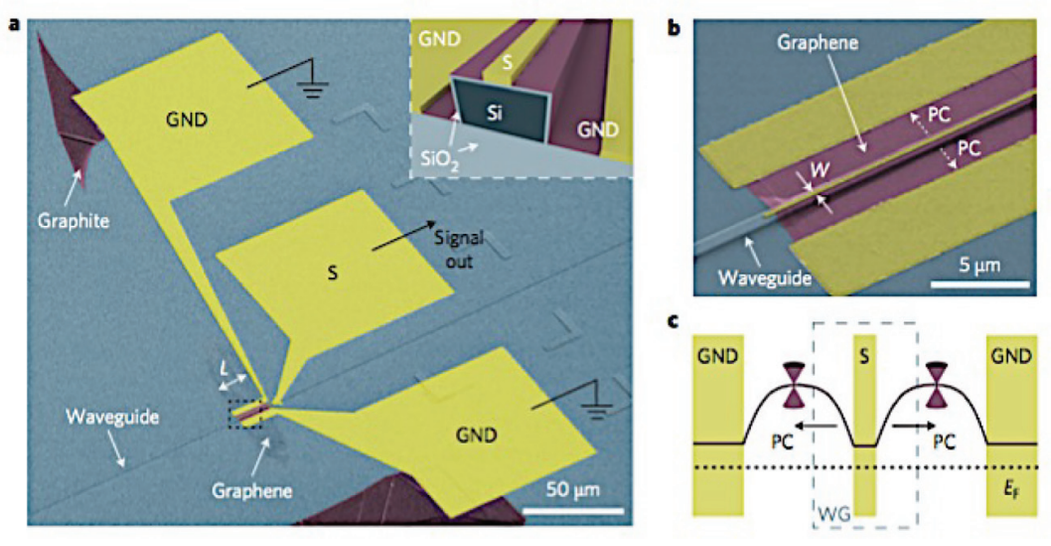

Figure 2. (a) Colored scanning electron micrograph of a waveguide-integrated graphene photodetector. The violet region represents graphene sheet. (b) enlarged view of the section highlighted by the black dashed rectangle in a. (c) Schematic illustration of the band diagram [24].

Gan et al. [29] achieved a photodetector which simultaneously exhibited high responsibility, high speed, and broadband spectral bandwidth by using a metal-doped graphene junction coupled evanescently with the waveguide, as shown in **Figure 3**. The absorption performance of

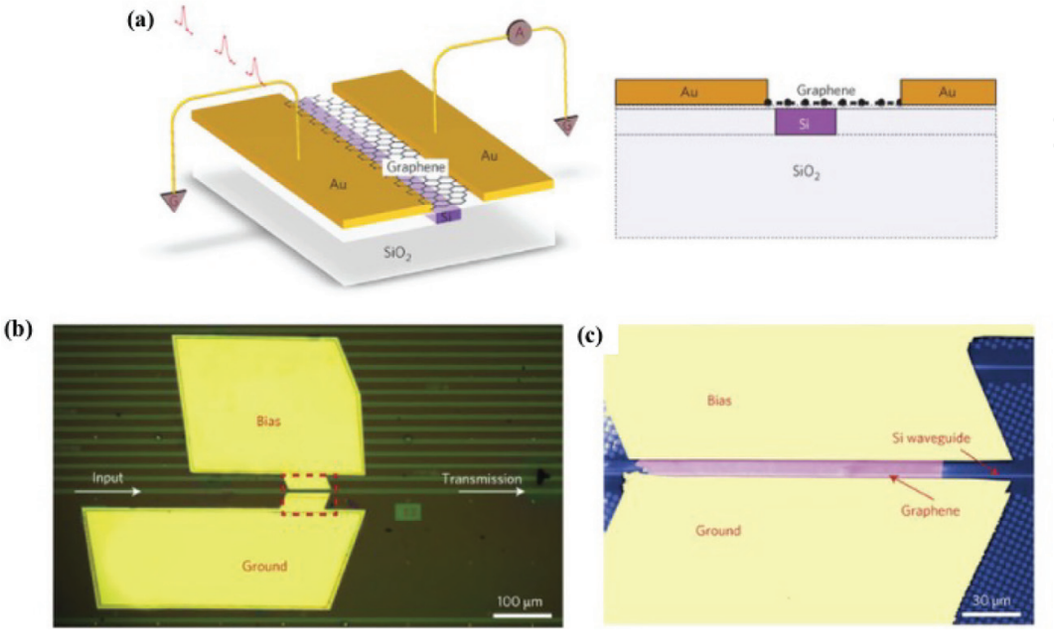

Figure 3. (a) Schematic of the waveguide-integrated graphene photodetector. (b) Optical microscopy top view of the device with a bilayer of graphene covering the waveguide. (c) SEM image showing the boxed region in (b) (false color), displaying the planarized waveguide (blue), graphene (purple) and metal electrodes (yellow) [29].

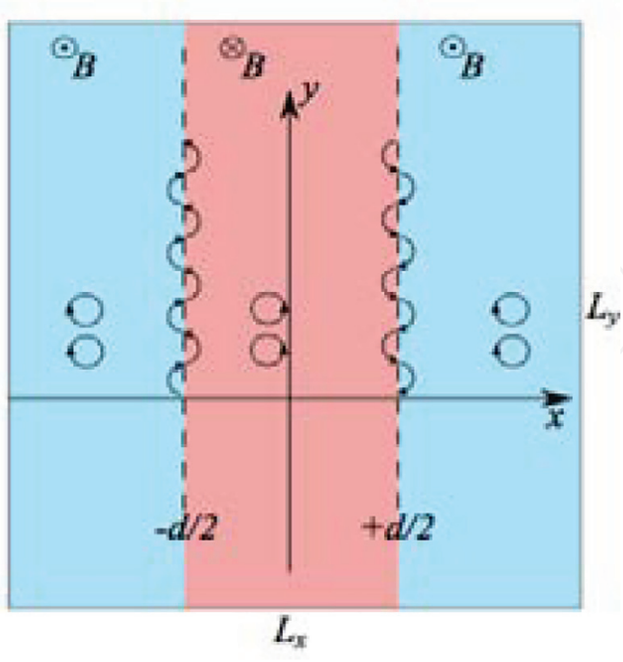

Figure 4. Schematic sketch of the MGW setup viewed from above. A magnetic field B is applied everywhere in the graphene plane except for the waveguide region $|x| < d/2$, where the field is reversed [32].

http://dx.doi.org/10.5772/intechopen.76796

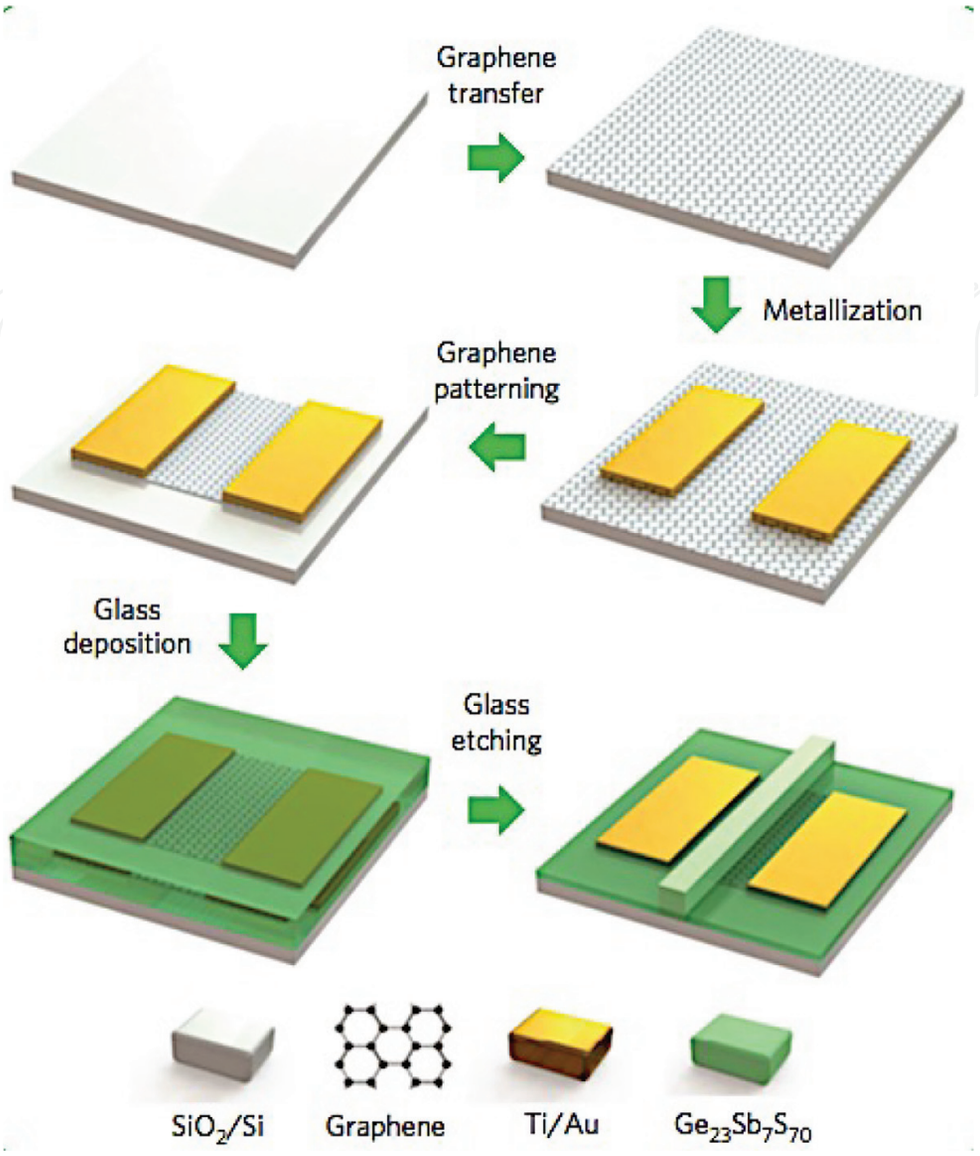

Figure 5. Schematic fabrication process flow to integrate chalcogenide glass photonic devices with graphene. Monolayer graphene had been grown on Cu foil by CVD method, which was then transferred onto the surface of target substrate by standard PMMA transformation process. Contract metals were then deposited and pattered on the surface of graphene. Subsequently, a standard electron-beam lithography process was adopted to patter graphene on the substrate. Then a glass film was deposited onto graphene surface by thermal evaporation, and the pattern of glass was defined by fluorine-based plasma etching [33].

graphene is improved by extending the length of graphene or by coupling graphene with a transverse-magnetic (TM) mode with a stronger evanescent field. Besides, the internal quantum efficiency of the photodetector can be improved by electrically grating the graphene layer to reshape the depth and location of the potential difference. In their research, they proved that graphene could be integrated with complementary-metal-oxide-silicon (CMOS), which made possible the realization of scalable ultra-high bandwidth graphene-based optical interconnectors.

The propagation of the electromagnetic field along the waveguide is summarized in two ways, which are known as transverse-electric (TE) and transverse-magnetic (TM) modes. Generally,

in the TE mode, the electric lines of flux are perpendicular to the axis of the waveguides. While in TM mode, the magnetic lines of flux are perpendicular to the axis of the waveguides. Normally, for waveguides using a single conductor, no transverse-electromagnetic (TEM) mode could be transmitted. Most research focus on the transmission of the TE mode, while Cohnitz et al. [32] investigated a magnetic graphene waveguide, in which a clean graphene is exposed to a static inhomogeneous magnetic field along one of the planar directions. As shown in **Figure 4**, when applying magnetic fields to a monolayer graphene, quantum modes exhibited like classical snake orbits near the field switch lines. While in the other regions far from these region, only Landau-quantized cyclotron orbits could be detected.

Usually, the integration of graphene with photonic devices relies on the transformation of exfoliated or delaminated or chemical vapor deposition (CVD)-fabricated 2D material onto pretreated devices, as shown in **Figure 5** [34]. However, the application of the transformation process is limited due to the shortcomings in uniformity and efficiency [35–37]. Most importantly, transferred 2D materials suffer from weak interaction with optical modes in pre-treated devices [37]. An atomic layer deposition (ALD) method has been adopted widely to obtain gate dielectric on graphene. Also, plasma-enhanced chemical vapor deposition (PECVD) could be another option for fabrication of silicon nitride on graphene. Last year, it was reported that the spin-coating process could be applied to directly fabricate the polymer waveguide modulator on graphene [38]. However, the fabrication technique of photonics devices integrating the graphene thin film needs to be improved for the difficulty of keeping the original properties of graphene after the following integrated progresses. Even though it's still a challenge to ensure the quality of integrated graphene up to date, the importance of optimized and the continuous study of graphene-based photonics devices, especially waveguides, are foreseen.

2. Electromagnetic properties of graphene-based waveguides

Most electromagnetic phenomena are governed by Maxwell equations, while the electromagnetic properties of materials are determined by two parameters, relative complex permittivity (ε) and relative complex magnetic permeability (μ), which describe the coupling of a material with incident electromagnetic energy. Normally, in the optical range, refraction index (n) is used as well to describe the macroscopic effective parameters of the material, and the refraction has as a relationship with relative complex permittivity (ε) and relative complex permeability (μ) the following:

$$n = \sqrt{\mu\varepsilon} \tag{1}$$

For most materials without magnetic properties, we treat $\mu = 1$ here. A conventional waveguide consists of a high-index core surrounded by a lower-index cladding.

2.1. Graphene's relative complex permittivity in vacuum

Graphene's optical properties can be determined by its relative complex permittivity. The equivalent in-plane component of graphene's relative permittivity is given by:

$$\varepsilon(\omega) = 1 + \frac{i\sigma(\omega)}{\omega\varepsilon_0 d} \tag{2}$$

where d is the thickness of the graphene layer, ε_0 is relative complex permittivity in vacuum ($\varepsilon_0 = 8.854$ F/m), ω is the optical frequency, and σ is graphene's optical conductivity. By using the Kubo method, we can calculate the optical conductivity (σ) which consists of intraband (σ_{intra}) and interband ($\sigma'_{inter} + i\sigma''_{inter}$) [39], as shown in **Figure 6**, thus:

$$\sigma_{total} = \sigma_{intra} + \sigma'_{inter} + \sigma''_{inter} \tag{3}$$

where

$$\sigma_{intra} = \sigma_0 \frac{4E_F}{\pi} \frac{1}{\hbar(\Gamma_1 - i\omega)} \tag{4}$$

$$\sigma'_{inter} = \sigma_0 \left[1 + \frac{1}{\pi} \tan^{-1}\left(\frac{\hbar\omega - 2E_F}{\hbar\Gamma_2}\right)\right] - \frac{1}{\pi} \tan^{-1}\left(\frac{\hbar\omega + 2E_F}{\hbar\Gamma_2}\right) \tag{5}$$

$$\sigma''_{inter} = -\sigma_0 \frac{1}{2\pi} In\left[\frac{(2E_F + \hbar\omega)^2 + (\hbar\Gamma_2)^2}{(2E_F - \hbar\omega)^2 + (\hbar\Gamma_2)^2}\right] \tag{6}$$

here, $\sigma_0 = e^2 4\hbar \cong 60.8$ μS is the universal optical conductance, E_F is the Fermi level of graphene, $\hbar$ is Planck's constant, and $\Gamma_1 = 8.3 \times 10^{11} s^{-1}$ and $\Gamma_2 = 10^{13} s^{-1}$ are relaxation rates at room temperature associated with the interband and intraband transitions, respectively.

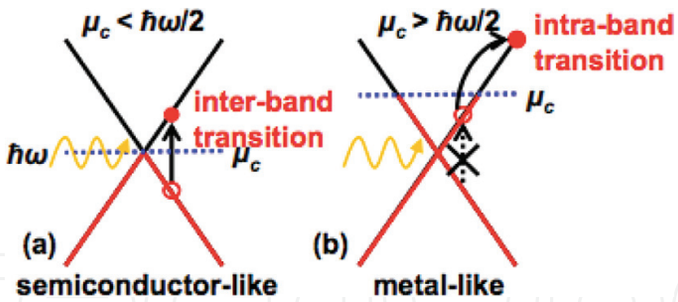

Figure 6. (a) Interband transition and (b) intraband transition in graphene [39].

Obviously, relative permittivity of this kind of waveguide is related to the conductivity of graphene, which would further influence the dispersion properties of the whole structure. When integrating graphene into the waveguide, the surface plasmon dispersion of graphene is strongly modified by the metal and other dielectric substrates; thus, the transmission of the incident electromagnetic wave in the waveguide is affected as well [40]. The characteristic plasmon dispersion relationship could be obtained by the following equation for the structure as described in **Figure 7(a)**:

$$\varepsilon_3 \frac{\varepsilon_4 + \varepsilon_3 \tanh qd_3}{\varepsilon_3 + \varepsilon_4 \tanh qd_3} + \varepsilon_2 \frac{\varepsilon_1 + \varepsilon_2 \tanh qd_2}{\varepsilon_2 + \varepsilon_1 \tanh qd_2} = -i\frac{q}{\omega}\sigma(q, \omega) \tag{7}$$

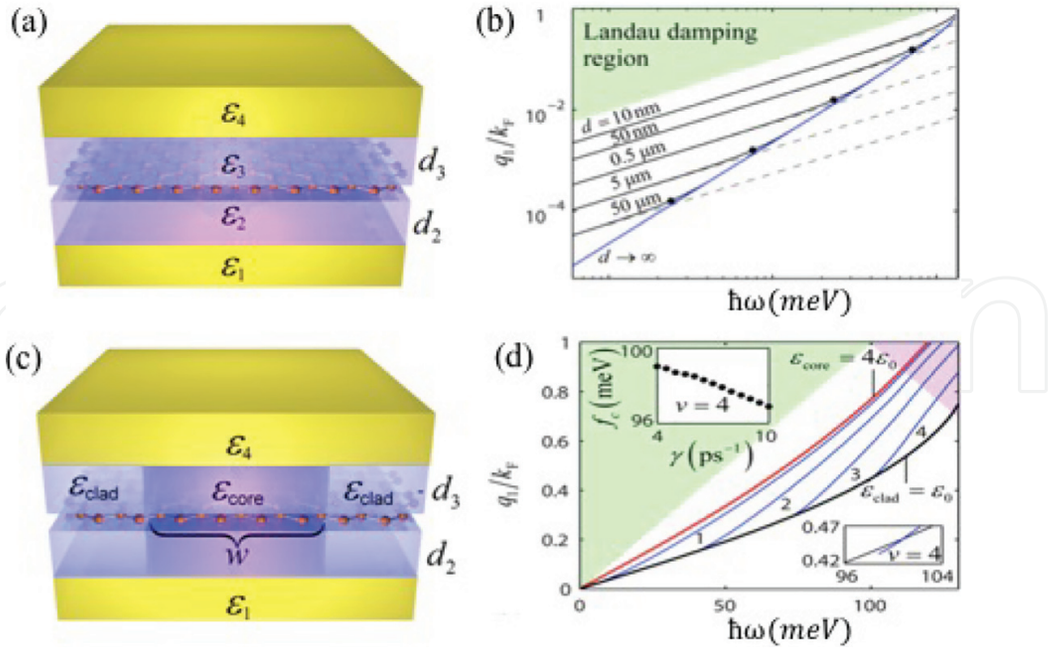

Figure 7. (a) Planar waveguide, and (c) non-planar rectangular waveguide. Dispersion characteristics of planar (b) and non-planar (d) waveguides [41].

for which the explanation of permittivity could be found in the **Figure 7(a)**. It should be noted here that the equation shows a good approximation when the thickness is much thicker than the skin depth [41]. As shown in **Figure 7(b)**, an enhanced confinement and an increased propagation distance can be obtained by adopting a metal slab within a certain spectral region. However, only the plasmonic field in the direction perpendicular to the surface could be confined to the model of **Figure 7(a)**. By adopting a non-planar structure as shown in **Figure 7 (c)**, 2D confinement could be obtained due to the dielectric boundaries in the other direction, of which the dispersion relationship could be obtained by an effective index method.

Graphene's relative permittivity can be easily tuned by electrostatic gating or chemical doping, which makes it easier to be applied for Talbot effect than metal-based devices [42]. Plasmonic Talbot carpets were experimentally obtained by using surface plasmon polariton (SPP) launching gratings, and a sub-wavelength focal spot can obtained.

2.2. The complex refraction index of graphene based waveguides

Borini's group estimated the optical index of graphene in visible range by dealing with universal optical conductivity and measured the optical spectrum within the framework of Fresnel's coefficient calculation [43]. Reflectometry is another method to acquire the reflection properties so as to obtain an average index over a broadband range by fitting the spectrum. Xu's group [44] calculated the complex refraction index of graphene at 1550 nm through reflectivity measurement on a SiO_2/Si substrate. And as reported by Wang [45], Notle's group applied picometrology to measure the refraction of graphene on thermal oxide on silicon at 488, 532, and 633 nm, respectively, in which the strong dispersion of the graphene index was observed in an optical range.

http://dx.doi.org/10.5772/intechopen.76796

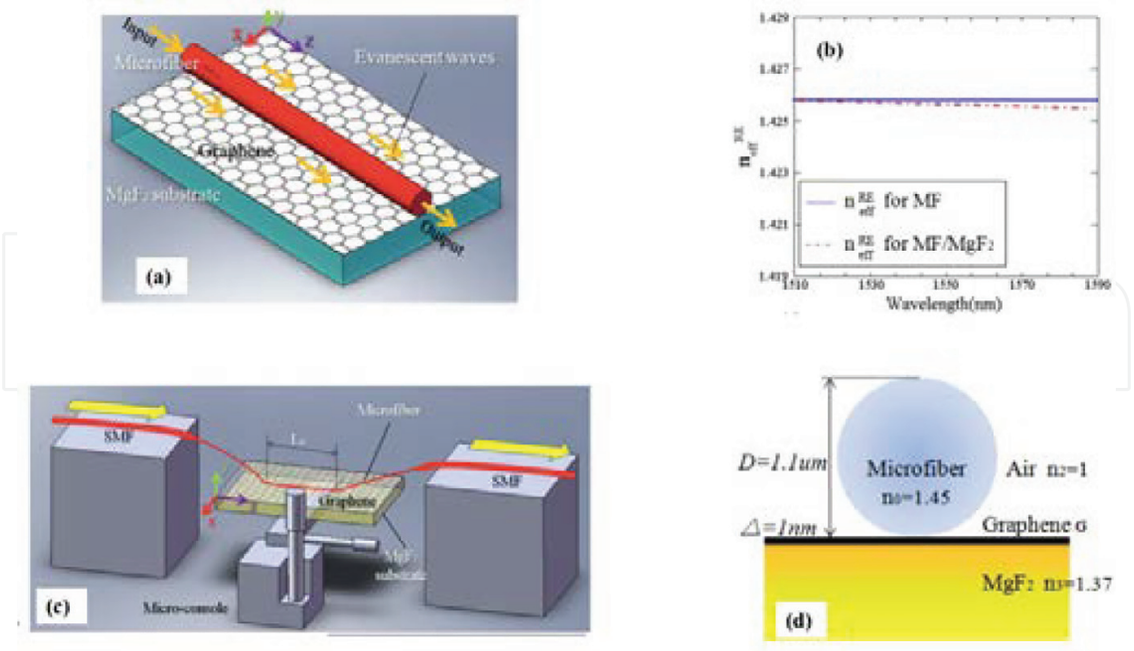

Figure 8. (a) Schematic diagram of the structure for the light propagating along the GMFW (red: Single mode fiber, white: Monolayer graphene, cyan: MgF_2 substrate). The orange arrows show the transmitting direction of the evanescent waves. (b) neffRE of the microfiber (blue solid) and the microfiber on MgF_2 (red dashed). (c) the experimental details of the GMHW. (d) Geometry of the cross-section of the GMHW [46].

However, in most conditions, graphene is regarded as a boundary condition when integrated into a waveguide due to the difficulty in a complex refraction index, while permittivity is regarded as a fundamental issue in graphene-based modern integrated photonics and devices. Yao's group [46] used a microfiber-based Mach-Zehnder interferometer to obtain the complex refraction index of the graphene waveguide from 1510 to 1590 nm, as shown in **Figure 8**. In this method, the microfiber acts as an effective mean to launch and collect the evanescent signal for the waveguide, for which, on the other hand, the contact length can adjusted if needed. As the results shown in **Figure 8(b)**, the complex refraction index of graphene-based waveguide varies from $2.91 - i3.92$ to $3.81 - i14.64$ in the experimental-range wavelength from 1510 to 1590 nm.

2.3. The tunability of graphene permittivity

When model graphene is infinitely thin, local two-sided surfaces with conductivity σ could be obtained based on Kubo function as the following:

$$\sigma(\omega, \mu_c, \Gamma, T) = \frac{je^2(\omega - j2\Gamma)}{\pi\hbar^2} \times \left\{ \begin{array}{l} \dfrac{1}{(\omega - j2\Gamma)^2} \displaystyle\int_0^\infty \varepsilon \left[\frac{\partial f_d(\varepsilon)}{\partial \varepsilon} - \frac{\partial f_d(-\varepsilon)}{\partial \varepsilon} \right] d\varepsilon \\ \\ - \displaystyle\int_0^\infty \left[\frac{f_d(-\varepsilon) - f_d(\varepsilon)}{(\omega - j2\Gamma)^2 - 4(\varepsilon/\hbar)^2} \right] d\varepsilon \end{array} \right\} \tag{8}$$

where ω is radiated frequency, μ_c is chemical potential, Γ refers to the phenomenological scattering rate that is assumed to be independent of energy, and T is temperature.

$$\mu_c = \hbar V_F \sqrt{\frac{\pi \varepsilon_{ox}}{e d_{ox}} (V - V_D)} \tag{9}$$

where V_F stands for Fermi velocity, ε_{ox}, d_{ox} corresponds to the permittivity and thickness of the dielectric, respectively, V_D is the Dirac voltage, and V is the externally applied voltage. Obviously, the chemical potential could be strongly tuned by the applied gate voltage, which, as a result, would impact the refraction index. Xu's group used the reflectivity measurement to obtain the complex refraction index of graphene on SiO_2/Si, which could be tuned by gate electric voltage, which agreed well with the Kubo function [44].

As shown in **Figure 9**, the real and imaginary part of the conductivity of graphene display a relationship with wavelength in the mid-infrared range [47]. Besides, the chemical potential which attributes the carrier density in graphene plays a critical role in controlling the conductivity. When $\hbar\omega > 2|\mu_c|$, the optical absorption of graphene is related to the real part of conductivity, which comes from the interband transition. Obviously, photocarriers are generated during the transition process, which could be used in applications such as photo-detection or modulators. While for $\hbar\omega < 2|\mu_c|$, the conductivity of graphene could be explained by Pauli's blocking theory. Thus, an electrostatic grating is always applied to adjust the chemical potential, and thus to tune the absorption of graphene, which lies as the principle to design optical modulators. Moreover, it's displayed in **Figure 9** that the imaginary part of intraband and interband conductivity has the opposite sign, which plays a critical role in determining whether the TE or TM mode could be propagated in graphene, which is always used in a polarizer.

2.4. Graphene integrated with nonlinear substrates

When integrating graphene with a nonlinear substrate, the relative complex permittivity of the substrate (ε_{sub}) could be explained by the following equation named Kerr-type medium [48]:

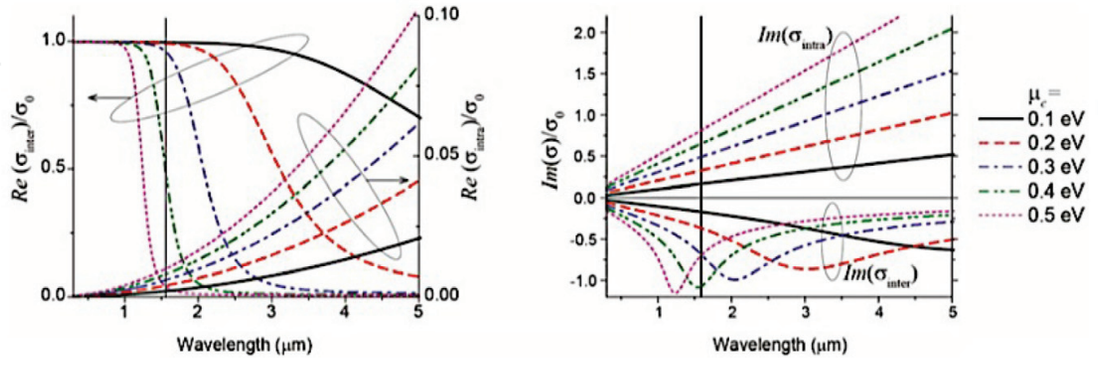

Figure 9. Interband (solid lines) and intraband (dashed lines) contribution to the dynamic conductivity in graphene. The vertical black line marks the telecommunication wavelength of λ = 1.55 μm [47].

$$\varepsilon_{sub} = \varepsilon_L + \alpha E^2 \tag{10}$$

where ε_L corresponds to the relative complex permittivity of substrate under linear incidence and E corresponds to the external incident electric field. Besides, graphene with conductivity of σ_g is treated as boundary here considering a one-atom scale thickness (**Figure 10**).

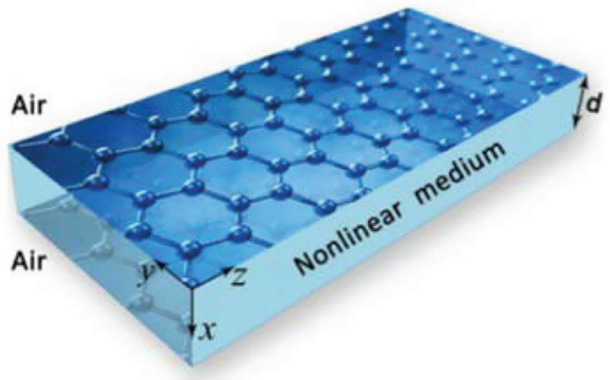

Figure 10. Schematic of waveguide constituted by graphene and nonlinear substrate [48].

For TM polarization with propagation constant β, three field components, *Ex*, *Ez*, and *Hy*, magnetic field ***H*** and electrical field ***E*** satisfy the following equations:

$$H = H_y y \tag{11}$$

$$E = E_x x + E_z z \tag{12}$$

$$\frac{dE_z}{d_x} = i\omega\mu_0 H_y + i\beta E_x \tag{13}$$

$$i\beta H_y = -i\omega\varepsilon_0\varepsilon E_x \tag{14}$$

$$\frac{dH_y}{dx} = i\omega\varepsilon_0\varepsilon E_z \tag{15}$$

where ε_0 and μ_0 correspond to electric permittivity and magnetic permeability in the vacuum, exactly as $\varepsilon_0 = 8.854 \times 10^{-12}\mathrm{F/m}$, $\mu_0 = 4\pi \times 10^{-7}\mathrm{H/m}$. When integrating graphene at the top of the Kerr-type substrate, we get:

$$\varepsilon^2 E_x^2 = \frac{\beta^2}{\omega^2\varepsilon_0^2} H_y^2 \tag{16}$$

$$E_x^2 = \left(\varepsilon - \varepsilon_L - \alpha E_z^2\right)/\alpha \tag{17}$$

Thus, we further get:

$$\varepsilon^3 - \left(\varepsilon_L + \alpha E_z^2\right)\varepsilon^2 - \frac{\alpha\beta^2}{\omega^2\varepsilon_0^2}H_y^2 = 0 \tag{18}$$

By a mathematical transformation, we can finally get the discriminant of permittivity ε:

$$\Delta = -\left(\varepsilon_L + \alpha E_z^2\right)^3 \frac{\alpha\beta^2}{\omega^2\varepsilon_0^2}H_y^2 - 27\frac{\alpha^2\beta^4}{\omega^4\varepsilon_0^4}H_y^4 < 0 \tag{19}$$

if $\Delta < 0$, then there is only one solution for ε. The equation is useful when we numerically calculate permittivity in the relaxation method. We can get permittivity through its real root. In particular, the nonlinear conductivity of graphene cannot be ignored any more under this condition, which can be expressed as:

$$\sigma_g = \sigma_L + \sigma^{NL}|E_\tau|^2 \tag{20}$$

where E_τ is the tangential component of the electric field and σ^{NL} contributes to nonlinear conductivity:

$$\sigma^{NL} = -i\frac{3}{8}\frac{e^2}{\pi\hbar^2}\left(\frac{eV_F}{\mu_c\omega}\right)^2\frac{\mu_c}{\omega} \tag{21}$$

in which V_F stands for Fermi velocity. It should be noted here that the conductivity of graphene is regarded as Drude type only in THz and far IR range.

3. Applications

Graphene could be an ideal option to meet the increasing demand of high-performance optoelectronics or some other communication components when the incident wave is confined along the thin film surface [49]. The 2D structure of graphene and the planar configuration of silicon photonics are inherently compatible with each other [47]. Normally, the maximum absorption in the monolayer graphene integrating at the dielectric surface is about 10~20%, which would not make a big difference even applying highest practically achievable carrier concentrations [8]. This character could be enhanced when incorporating graphene on the surface of a passive silicon dielectric waveguide, and the modulation depth could be as high as 50% when applying voltage to the graphene sheet.

The application of graphene-based waveguides can be summarized to be modulators, detectors, sensors, polarizers and some other applications, as discussed in detail through the following.

3.1. Graphene-based waveguide integrated modulators

Thanks to the outstanding properties of graphene in conductivity, current density, and charge mobility, graphene-based waveguides are supposed to have promising potentials in applications

such as unrivaled speed, low driving voltage, small physical footprints, and low power consumption [50], which can further be utilized in telecommunications and optoelectronics. While several graphene-based waveguides have been investigated, it still remains a challenge to combine graphene with plasmonic waveguides. How to control the intensity, phase, and polarization of the electromagnetic wave in an optical range through the waveguide attracts a lot of interest. When integrating graphene into a waveguide, the waveguide mode propagates along and is confined near a graphene sheet, which is regarded as the most promising for on-chip information processing. However, we have to admit here that even though the atomic thickness of graphene gives rise to lots of advantages, there are several challenges to deal with in such a device, such as unavoidable power consumption, slowdown response, and lower modulation depth.

Due to the tunable bandgap of graphene, waveguide modulators could be formed with broad flexibility [8, 50]. Besides, the carried density of graphene could be tuned manually through external gate voltage [51, 52], chemical doping [53, 54], and optical (laser) excitation [55]. As a result, the refraction index and the permittivity could be adjusted. It is worth mentioning here that the response of graphene in an optical range could be tuned by substrates as well [56], which may induce a bandgap opening in epitaxial graphene [57]. The transmission of 1.53 μm photons through the waveguide at a varied drive voltage is shown in **Figure 11**, which has been divided into three different regions from −6 to 6 V and the corresponding band structures are shown as insets. In the left region with drive voltage bellow −1 V, the Fermi level (E_F) was lower than half photonic energy ($\frac{1}{2}\hbar v$), and no electrons were available for further interband transition. In the middle region for drive voltage ranging from −1 to 3.8 V, the Fermi level was close to Dirac point; thus, it is possible for electrons in occupied regions transiting to unoccupied regions. In other words, graphene sheets showed potential in phonon absorbing, indicating its modulation ability. In the third region from 3.8 to 6 V, the transition was blocked again since all the electron states which were in resonance while the incident phonons were occupied.

Grigorenko's group reported a hybrid graphene-plasmon waveguide modulator for promising applications in telecom as shown in **Figure 12**, whose modulation depth was comparable with silicon-based waveguide modulators, showing a promising future for optical communication [50].

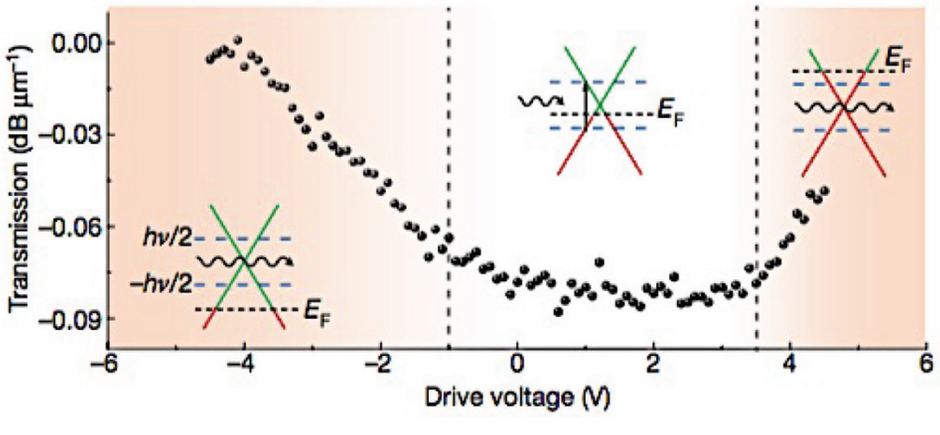

Figure 11. Displays the transmission of 1.53 μm photons through the waveguide at different drive voltages.

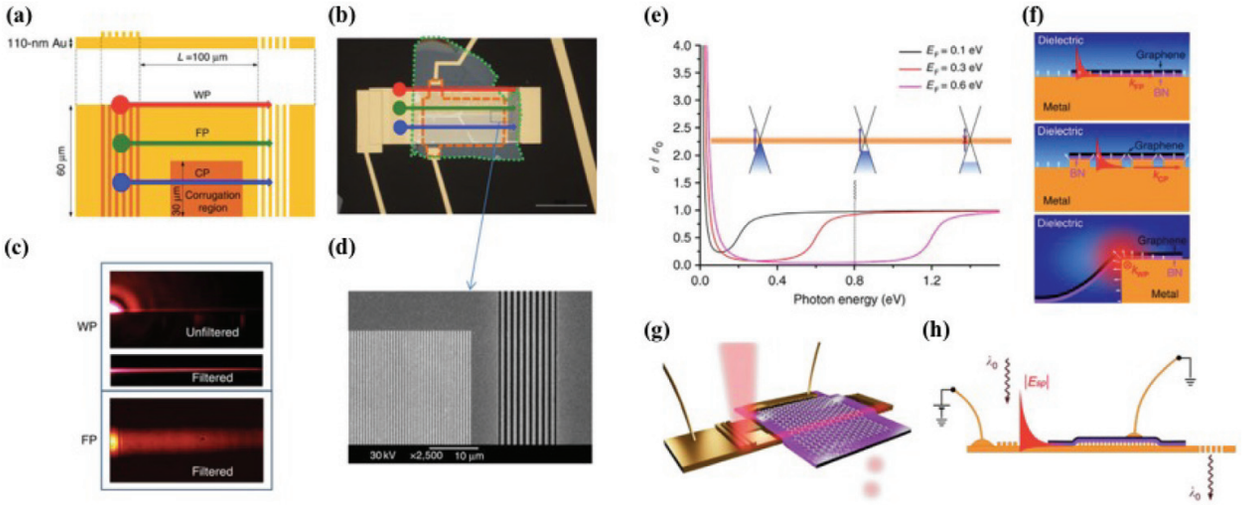

Figure 12. (a) The schematics of the hybrid graphene plasmonic waveguide modulators. (b) The optical micrograph of a typical hybrid graphene plasmonic modulator studied in this work. (c) Leakage radiation detection of wedge, upper panel, and flat, lower panel, plasmon-propagating modes. (d) A scanning electron micrograph of an area shown in b by the dotted box that shows corrugated waveguide and the semitransparent decoupling grating. (e) Optical Pauli blocking expressed in terms of graphene relative conductivity. (f) Sketches of three types of plasmonic modes under investigation —flat, corrugated and wedge plasmons. (g) 3D rendering of the experiment with the wedge plasmon mode. (h) The schematic of experiment where non-transparent grating couples light into plasmon modes [50].

The conductivity of graphene related to Fermi energy depends on the applied voltage between graphene layers and the thickness and permittivity of the dielectric layer located between two graphene layers. Asgari's group [58] applied bias voltage V_b between two graphene layers which leads to an equal increase in electron density in the top layer and hole density in the bottom layer, as shown in **Figure 13**. Therefore, the absolute values of Fermi energies (E_F) in both graphene layers were identical but of opposite signs. Voltage application caused a potential difference between two graphene layers. Actually, when applying bias voltage between two graphene sheets, a capacitor effect could be observed. Besides, charge density in both sheets would increase with bias voltage, as well as Fermi energy. As a result, intraband conductivity would increase, while interband conductivity decreases.

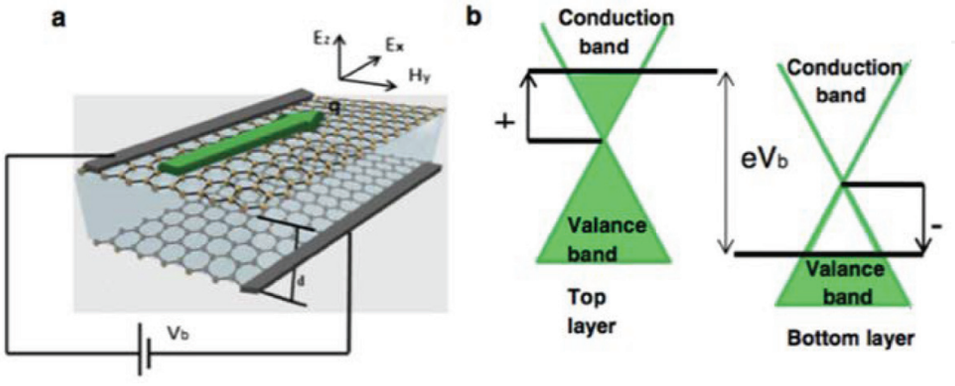

Figure 13. (a) Schematic illustration of the two-graphene layer structure and direction of electric and magnetic field components in TM mode. (b) The band scheme of the structure at bias voltage V_b [58].

However, Murphy's group [8] designed a THz modulator formulated by setting large graphene sheets at the middle of two SiO_2 layers (300 nm) with Si wafers on both their sides based on ridge waveguides, as shown in the figure above. When applying voltage to graphene sheets, light-matter interaction could be modulated. As a result, the modulation depth could be achieved as high as 50%. Obviously, the carrier concentration in the graphene sheet would be modified by adjusting gate voltage. When voltage was guided through the graphene sheet in the waveguide, the electric field would penetrate into the graphene sheet and lead to absorption due to free carriers in the graphene sheet.

3.2. Graphene-based waveguide photodetectors

Conventionally, low band-gap semiconductors such as HgCdTe alloys or quantum-well and quantum-dot structures on III-V materials are adopted to formulate mid-infrared detectors [59]. With electrical tunability in light absorption and ultra-fast photo-response, graphene is regarded as a promising candidate for high-speed photo-detection applications [9]. It has been approved that graphene-based waveguide photodetectors could be applied from 300 nm to 6 μm or even longer [4]. It should be noted here that a dark current range may occur due to the gapless inherent properties of graphene, which should be avoided in practical application [60]. Thus, chemical potential must be tuned near the Dirac energy to ensure that incident field is illuminated to the graphene thin film.

Wang et al. [30] integrated monolayer graphene into a silicon optical waveguide on a silicon-on-insulator (SOI) from near-to-mid-infrared operational range, which indicated that the combination of the graphene silicon structure made it possible to overcome the shortcomings of the traditional junction-less photodetectors. As a result, a much higher sensitivity could be expected in graphene-based waveguides. The transverse electric mode light (~10 μm spot size) was coupled into the waveguide via a focusing sub-wavelength grating. Avouris' group [60] reported an efficient photodetection of the waveguide based on graphene, as shown in **Figure 14**, which shows gate-dependent response, and the response is nearly linear on the entire device of 10 mV. And the measurement from network analyzer showed the relative A.C photo-response, which could be further improved by applying a bias within the photocurrent generation path.

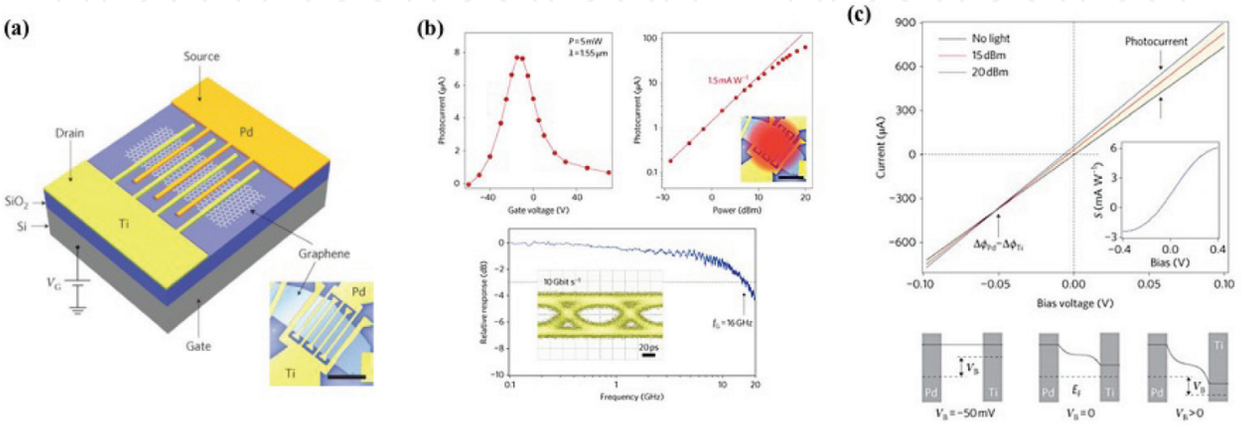

Figure 14. Photocurrent generation, high-frequency characterization of the MGM photodetector, and operation of the MGM photodetector at a data rate of 10 Gbit·s^{-1} with 1.55 μm light excitation [60].

However, it's difficult to fabricate these materials which are challenging to operate at room temperature till now. Choi's group [61] integrated graphene with a Bi_2Se_3 heterostructure, in which graphene functioned as high mobility charge transport layers and Bi_2Se_3 functioned as a broadband IR absorber supplying holes in graphene. The graphene-Bi_2Se_3 structure showed broadband absorption and high-intensity response at room temperature.

3.3. Graphene-based waveguide sensors

Graphene is used in sensors, thanks to its unique electric properties, which show great potential in chemical or biology sensors. Among all varieties of chemical gas sensors, photonics gas sensors have advantages because of their high sensitivity and stability. Graphene plays a critical role in gas sensing due to the sensitivity of carried density to environment [62]. Graphene's conductivity can be changed drastically by adsorbed gas molecules which serve as charge carrier donors or acceptors to modulate the local carrier concentration of graphene. Cheng and Goda [63] conducted a graphene-based waveguide to measure NO_2 gas concentration based on germanium and silicon substrates, respectively, as shown in **Figure 15**, where sensitivity was about 20 times higher than that of the graphene-covered microfiber sensor. Li et al. [64] demonstrated a single graphene-based waveguide which simultaneously provides optical modulation and photodetection. For developing sensitive photonic gas sensors, it is important to consider the interaction of propagating light in the waveguide to the top graphene layer. Xiang's group [65, 66] conducted a series work on graphene waveguide bio-sensors, by coupling graphene surface plasmon polaritons (SPPs) and planar waveguides to realize the ultrasensitive response. The SPPs produced by graphene could be used for bio-sensors since the SPPs are extremely sensitive to changes in the dielectric constant; even small changes in molecular density could be detected [67]. Graphene-based waveguides could overcome the shortcomings in traditional bio-sensors such as low speed, more time, and insufficient sensitivity.

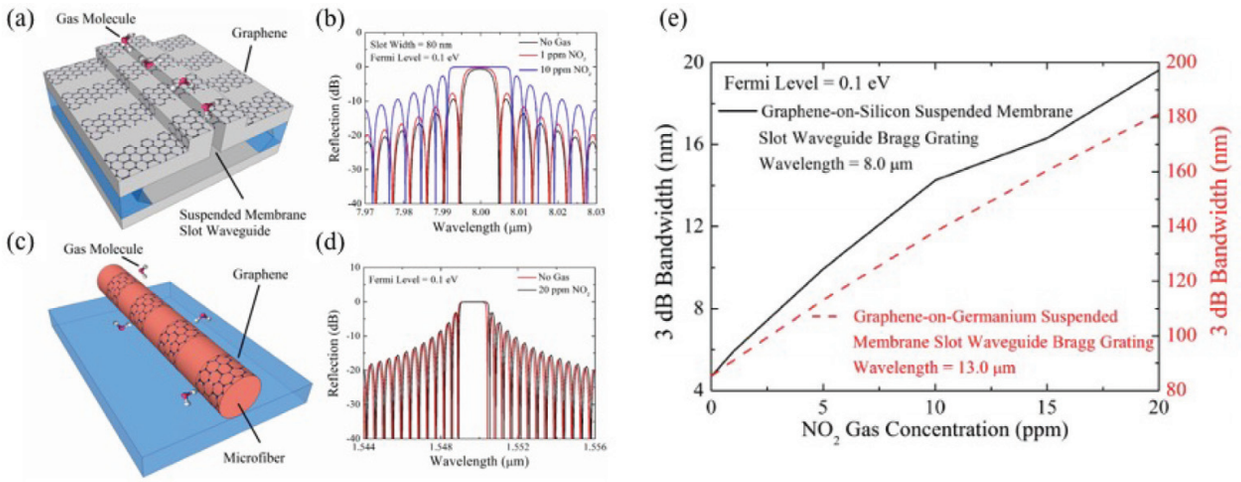

Figure 15. Design of graphene on silicon (GoG) and suspended membrane slot waveguide (SMSW) Bragg grating gas sensor in comparison with the graphene-covered microfiber Bragg grating gas sensor. The calculated 3 dB bandwidth of the proposed GoS-SMSW Bragg gratings as a function of the NO_2 gas concentration was shown [63].

http://dx.doi.org/10.5772/intechopen.76796

3.4. Other waveguides

Usually, a fixed optical device works only on one particular polarization state, either the TE or the TM polarization state [68]. By coating silicon waveguides with graphene, a versatile polarizer works in two operation modes, which were based on the different effective mode index variations [69].

Waveguide integrated with graphene has nonlinear parameters which depend strongly on the Fermi level of graphene. It has been demonstrated that Integrating graphene with slot waveguide would benefit non-linear properties, owing to the interaction enhancement between graphene and incident electromagnetics [70].

When integrating graphene with nonlinear substrates on one or both sides, the surface plasmons' (SPs) localization length increased while their propagation length (PL) remained unchanged compared with the typical graphene waveguide [71, 72].

4. Conclusion

In conclusion, due to its unique electric and electromagnetic properties, graphene acts as a promising candidate for photonics and communication component of high performance. Especially, integrating graphene with waveguides makes it possible to overcome shortcomings such as limited bandwidth, inevitable cross-talk, high energy consumption, and expensive cost in conventional devices. Furthermore, the gapless linear dispersion of Dirac fermions makes it possible for graphene integrated with other substrates to formulate modulators, polarizers, broadband waveguides, photodetectors, bio-sensors, and so on. And the permittivity of graphene-based waveguides could be calculated based on Maxwell's function, even integrating with nonlinear substrates. The application of graphene waveguides expands the broadband range, from 300 nm to 6 μm or even longer. By tuning the carrier density of graphene through external gate voltage, chemical doping, or optical excitation, the relative complex permittivity of graphene is tuned. Thus, graphene waveguide modulators could be formed which adjusts absorption and modulation depth and so on. Besides, graphene waveguides show potential in fast and high-response detection and chemical sensing. The recent development in graphene synthesis and photonics components' fabrication technique ensures the compatibility in the integrated electronics platform, which shows a bright prospect in the near future.

Author details

Xianglian Song, Xiaoyu Dai and Yuanjiang Xiang*

*Address all correspondence to: xiangyuanjiang@126.com

International Collaborative Laboratory of 2D Materials for Optoelectronic Science and Technology of Ministry of Education, College of Optoelectronic Engineering, Shenzhen University, China

References

[1] Youngblood N, Chen C, Koester SJ, Li M. Waveguide-integrated black phosphorus photodetector with high responsivity and low dark current. Nature Photonics. 2015;**9**:247-252. DOI: 10.1038/nphoton.2015.23

[2] Ding Y, Guan X, Hu H. Efficient electro-optic modulation in low-loss graphene-plasmonic slot waveguides. Nanoscale. 2017;**9**:15576-15581. DOI: 10.1039/C7NR05994A

[3] Gao X, Cui TJ. Spoof surface plasmon polaritons supported by ultrathin corrugated metal strip and their applications. Nanotechnology Reviews. 2015;**4**:239-258. DOI: 10.515/ntrev-2014-0032

[4] Schuler S, Schall D, Neumaier D. Controlled generation of a p-n junction in a waveguide integrated graphene photodetector. Nano Letters. 2016;**16**:7107-7112. DOI: 10.1021/acs.nanolett.6b03374

[5] Chen M, Sheng P, Sun W. A symmetric terahertz graphene-based hybrid plasmonic waveguide. Optics Communications. 2016;**376**:41-46. DOI: 10.1016/j.optcom.2016.05.020

[6] Kovacevic G, Yamashita S. Waveguide design parameters impact on absorption in graphene coated silicon photonic integrated circuits. Optics Express. 2016;**24**:3584-3591. DOI: 10.1364/OE.24.003584

[7] Kou R, Tanabe S, Tsuchizawa T. Characterization of optical absorption and polarization dependence of single-layer graphene integrated on a silicon wire waveguide. Japanese Journal of Applied Physics. 2013;**52**:060203. DOI: 10.7567/JJAP.52.060203

[8] Mittendorff M, Li S, Murphy TE. Graphene-based waveguide-integrated terahertz modulator. ACS Photonics. 2017;**4**:316-321. DOI: 10.1021/acsphotonics.6b00751

[9] Shiue RJ, Gao Y, Wang Y. High-responsivity graphene-boron nitride photodetector and autocorrelator in a silicon photonic integrated circuit. Nano Letters. 2015;**15**:7288-7293. DOI: 10.1021/acs.nanolett.5b02368

[10] Ooi KJA, Leong PC, Ang LK. All-optical control on a graphene-on-silicon waveguide modulator. Scientific Reports. 2017;**7**:12748. DOI: 10.1038/s41598-017-13213-6

[11] Low T, Chaves A, Caldwell JD. Polaritons in layered two-dimensional materials. Nature Materials. 2016;**16**:182-194. DOI: 10.1038/nmat4792

[12] Nemilentsau A, Low T, Hanson G. Anisotropic 2D materials for tunable hyperbolic Plasmonics. Physical Review Letters. 2016;**116**:066804–5. DOI: 10.1103/PhysRevLett.116.066804

[13] Novoselov KS, Geim AK, Morozov AV. Electric field effect in atomically thin carbon films. Science. 2004;**306**:666-669. DOI: 10.1126/science.1102896

[14] Meyer JC, Geim AK, Mi K. The structure of suspended graphene sheets. Nature. 2007;**446**:60-63. DOI: 10.1038/nature05545

[15] Youngblood N, Li M. Integration of 2D materials on a silicon photonics platform for optoelectronics applications. Nano. 2017;**6**:1205-1218. DOI: 10.1515/nanoph-2016-0155

[16] Singh V, Joung D, Zhai L. Graphene based materials: Past, present and future. Progress in Materials Science. 2011;**56**:1178-1271. DOI: 10.1016/j.pmatsci.2011.03.003

[17] Hecht DS, Hu L, Irvin G. Emerging transparent electrodes based on thin films of carbon nanotubes, graphene, and metallic nanostructures. Advanced Materials. 2011;**23**:1482-1513. DOI: 10.1002/adma.201003188

[18] Nandamuri G, Roumimov S, Solanki R. Chemical vapor deposition of graphene films. Nanotechnology. 2010;**21**:145604. DOI: 10.1088/0957-4484/21/14/145604

[19] Edwards RS, Coleman KS. Graphene synthesis: Relationship to applications. Nanoscale. 2012;**5**:38-51. DOI: 10.1039/C2NR32629A

[20] Avouris P, Xia F. Graphene applications in electronics and photonics. MRS Bulletin. 2012; **37**:1225-1234. DOI: 10.1557/mrs.2012.206

[21] Sun Z, Martinez A, Wang F. Optical modulators with 2D layered materials. Nature Photonics. 2016;**10**:227-238. DOI: 10.1038/nphoton.2016.15

[22] Gan Q, Bartoli FJ, Kafafi ZH. Plasmonic-enhanced organic photovoltaics: Breaking the 10% efficiency barrier. Advanced Materials. 2013;**25**:2385-2396. DOI: 10.1002/adma.201203323

[23] Du W, Wang T, Chu HS. Highly efficient on-chip direct electronic–plasmonic transducers. Nature Photonics. 2017;**11**:623-627. DOI: 10.1038/s41566-017-0003-5

[24] Kim KS, Zhao Y, Jang H. Large-scale pattern growth of graphene films for stretchable transparent electrodes. Nature. 2009;**457**:706-710. DOI: 10.1038/nature07719

[25] De Arco LG, Zhang Y, Schienker CW. Continuous, highly flexible, and transparent graphene films by chemical vapor deposition for organic photovoltaics. ACS Nano. 2010; **4**:2865-2873. DOI: 10.1021/nn901587x

[26] Mikhailov SA. Electromagnetic response of electrons in graphene: Non-linear effects. Physica E: Low-dimensional Systems and Nanostructures. 2008;**40**:2626-2629. DOI: 10.1016/j.physe.2007.09.018

[27] Zhu H, Liu A, Shan F. One-step synthesis of graphene quantum dots from defective CVD graphene and their application in IGZO UV thin film phototransistor. Carbon. 2016;**100**: 201-207. DOI: 10.1016/j.carbon.2016.01.016

[28] Pospischil A, Humer M, Furchi MM. CMOS-compatible graphene photodetector covering all optical communication bands. Nature Photonics. 2013;**7**:892-896. DOI: 10.1038/nphoton.2013.240

[29] Gan X, Shiue RJ, Gao Y. Chip-integrated ultrafast graphene photodetector with high responsivity. Nature Photonics. 2013;**7**:883-887. DOI: 10.1038/nphoton.2013.253

[30] Wang X, Cheng Z, Xu K. High-responsivity graphene/silicon-heterostructure waveguide photodetectors. Nature Photonics. 2013;**7**:888-891. DOI: 10.1038/nphoton.2013.241

[31] Liu M, Zhang X. Silicon photonics: Graphene benefits. Nature Photonics. 2013;**7**:851-852. DOI: 10.1038/nphoton.2013.257

[32] Cohnitz L, Haeusler W, Zazunov A. Interaction-induced conductance from zero modes in a clean magnetic graphene waveguide. Physical Review B. 2015;**92**:085422. DOI: 10.1103/PhysRevB.92.085422

[33] Lin H, Song Y, Huang Y. Chalcogenide glass-on-graphene photonics. Nature Photonics. 2017;**11**:798-805. DOI: 10.1038/s41566-017-0033-z

[34] Liu LH, Zorn G, Castner DG. A simple and scalable route to wafer-size patterned graphene. Journal of Materials Chemistry. 2010;**20**:5041-5046. DOI: 10.1039/C0JM00509F

[35] Sun Z, James DK, Tour JM. Graphene chemistry: Synthesis and manipulation. Journal of Physical Chemistry Letters. 2011;**2**:2425-2432. DOI: 10.1021/jz201000a

[36] Tang Q, Zhou Z, Chen Z. Graphene-related nanomaterials: Tuning properties by functionalization. Nanoscale. 2013;**5**:4541-4583. DOI: 10.1039/C3NR33218G

[37] Yan Z, Peng Z, Sun Z. Growth of bilayer graphene on insulating substrates. ACS Nano. 2011;**5**:8187-8192. DOI: 10.1021/nn202829y

[38] Kleinert M, Herziger F, Reinke P. Graphene-based electro-absorption modulator integrated in a passive polymer waveguide platform. Optical Materials Express. 2016;**6**:1800-1807. DOI: 10.1364/OME.6.001800

[39] Kayoda T, Han JH, Takenaka M. Evaluation of chemical potential for graphene optical modulators based on the semiconductor-metal transition. In: IEEE 10th International Conference on Group IV Photonics, 2013. DOI: 10.1109/Group4.2013.6644446

[40] Kozina ON, Melnikov LA, Nefedov IS. Dispersion characteristics of hyperbolic graphene-semiconductors multilayered structure. In: Proceedings SPIE 9448, Saratov Fall Meeting 2014: Optical technologies in biophysics and medicine XVI; Laser physics and photonics XVI; and Computational biophysics. 2014. DOI: 10.117/12.2180053

[41] Lin I, Liu JM. Enhanced graphene plasmon waveguiding in a layered graphene-metal structure. Applied Physics Letters. 2014;**105**:011604. DOI: 10.1063/1.4889915

[42] Li K, Xia F, Wang M. Discrete Talbot effect in dielectric graphene plasmonic waveguide arrays. Carbon. 2017;**118**:192-199. DOI: 10.106/j.carbon.2017.03.047

[43] Bruna M, Borini S. Optical constants of graphene layers in the visible range. Applied Physics Letters. 2009;**94**:031901. DOI: 10.1063/1.3073717

[44] Xu F, Das S, Gong Y. Complex refractive index tunability of graphene at 1550 nm wavelength. Applied Physics Letters. 2015;**106**:031109. DOI: 10.1063/1.4906349

[45] Wang X, Chen Y, Nolte D. Strong anomalous optical dispersion of graphene: Complex refractive index measured by Picometrology. Optics Express. 2008;**16**:22105-22112. DOI: 10.1364/OE.16.022105

[46] Yao B, Wu Y, Wang Z. Demonstration of complex refractive index of graphene waveguide by microfiber-based Mach-Zehnder interferometer. Nature Photonics. 2013;**21**:29818-29826. DOI: 10.1364/OE.21.029818

[47] Koester S, Li M. Waveguide-coupled graphene optoelectronics. IEEE Journal of Selected Topics in Quantum Electronics. 2014;**20**:600021. DOI: 10.1109/JSTQE.2013.2272316

[48] Jiang X, Bao J, Zhang B. Dual nonlinearity controlling of mode and dispersion properties in graphene-dielectric plasmonic waveguide. Nanoscale Research Letters. 2017;**12**:395. DOI: 10.1186/s11671-017-2166-x

[49] Cheng B, Chen H, Jen Y. Tunable tapered waveguide for efficient compression of light to graphene surface plasmons. Scientific Reports. 2016;**6**:28799. DOI: 10.1038/srep28799

[50] Ansell D, Radko I, Han Z. Hybrid graphene plasmonic waveguide modulators. Nature Communications. 2015;**6**:8846. DOI: 10.1038/ncomms9846

[51] Vasko F, Zozoulenko I. Conductivity of a graphene strip: Width and gate-voltage dependencies. Applied Physics Letters. 2010;**97**:092115. DOI: 10.1063/1.3486178

[52] Hu H, Zhai F, Hu D. Broadly tunable graphene plasmons using an ion-gel top gate with low control voltage. Nanoscale. 2015;**7**:19493-19500. DOI: 10.1039/C5NR05175D

[53] Khan MF, Iqbal MZ, Iqbal MW. Improving the electrical properties of graphene layers by chemical doping. Science and Technology of Advanced Materials. 2014;**15**:055004. DOI: 10.1088/1468-6996/15/5055004

[54] Pi K, Han W, McCreary K. Manipulation of spin transport in graphene by surface chemical doping. Physical Review Letters. 2010;**104**:187201. DOI: 10.1103/PhysRevLett.104.187201

[55] Chen C, Park C, Boudouris B. Controlling inelastic light scattering quantum pathways in graphene. Nature. 2011;**471**:617-620. DOI: 10.1038/nature09866

[56] Jablan M, Buljan H, Soljačić M. Plasmonics in graphene at infrared frequencies. Physical review B. 2009;**80**:245435. DOI: 10.1103/PhysRevB.80.245435

[57] Zhou S, Gweon G, Fedorov A. Substrate-induced bandgap opening in epitaxial graphene. Nature Materials. 2007;**6**:770-775. DOI: 10.1038/nmat2003

[58] Doust S, Siahpoush V, Asgari A. The tunability of surface plasmon polaritons in graphene waveguide structures. Plasmonics. 2017;**12**:1633-1639. DOI: 10.1007/s11468-016-0428-6

[59] Zhang X, Yang S, Zhou H. Perovskite-erbium silicate nanosheet hybrid waveguide photodetectors at the near-infrared telecommunication band. Advanced Materials. 2017;**29**: 1604431. DOI: 10.1002/adma.201604431

[60] Mueller T, Xia F, Avouris P. Graphene photodetectors for high-speed optical communications. Nature Photonics. 2010;**4**:297-301. DOI: 10.1038/nphoton.2010.40

[61] Kim J, Park S, Jang H. Highly sensitive, gate-tunable, room temperature mid-infrared photodetection based on graphene-Bi_2Se_3 heterostructure. ACS Photonics. 2017;**4**:482-488. DOI: 10.1021/acsphotonics.6b00972

[62] Hwang T, Kim J, Kulkarni A. Graphene photo detector with integrated waveguide biochemical sensors. Sensors and Actuators B: Chemical. 2013;**187**:319-322. DOI: 10.1016/j.snb.2012.11.092

[63] Cheng Z, Goda K. Design of waveguide-integrated graphene devices for photonic gas sensing. Nanotechnology. 2016;**27**:505206. DOI: 10.1088/0957-4484/27/50/505206

[64] Youngblood N, Anugrah Y, Ma R. Multifunctional graphene optical modulator and photodetector integrated on silicon waveguides. Nano Letters. 2014;**14**:2741-2746. DOI: 10.1021/nl500712u

[65] Ruan B, Guo J, Wu L. Ultrasensitive terahertz biosensors based on Fano resonance of a graphene/waveguide hybrid structure. Sensors. 2017;**17**:1924. DOI: 10.3390/s17081924

[66] Wu L, Guo J, Xu H. Ultrasensitive biosensors based on long-range surface plasmon polariton and dielectric waveguide modes. Photonics Research. 2016;**4**:262-266. DOI: 10.1364/PRJ.4.000262

[67] Wijesinghe T, Premaratne M, Agrawal G. Low-loss dielectric-loaded graphene surface plasmon polariton waveguide based biochemical sensor. Journal of Applied Physics. 2015;**117**:213105. DOI: 10.1063/1.4922124

[68] Pei C, Yang L, Wang G. Broadband graphene/glass hybrid waveguide polarizer. IEEE Photonics Technology Letters. 2015;**27**:927-930. DOI: 10.1109/LPT.2015.2398352

[69] Hao R, Du W, Li E. Graphene assisted TE/TM-independent polarizer based on Mach-Zehnder interferometer. IEEE Photonics Technology Letters. 2015;**27**:1112-1115. DOI: 10.1109/LPT.2015.2408375

[70] Wang J, Cheng Z, Chen Z. High-responsivity graphene-on-silicon slot waveguide photodetectors. Nanoscale. 2016;**8**:13206-13211. DOI: 10.1039/C6NR03122F

[71] Hajian H, Soltani-Vala A, Kalafi M. Surface plasmons of a graphene parallel plate waveguide bounded by Kerr-type nonlinear media. Journal of Applied Physics. 2014;**115**:083104. DOI: 10.1063/1.4865435

[72] Yarmoghaddam E, Rakheja S. Dispersion characteristics of THz surface plasmons in nonlinear graphene-based parallel-plate waveguide with Kerr-type core dielectric. Journal of Applied Physics. 2017;**122**:083101. DOI: 10.1063/1.4991674